

Published in final edited form as:

*Nat Biomed Eng.* 2018 June 18; 2: 649–656. doi:10.1038/s41551-018-0248-4.

## First-in-human study of the safety and viability of intraocular robotic surgery

T. L. Edwards<sup>1,2</sup>, K. Xue<sup>1,2</sup>, H. C. M. Meenink<sup>3</sup>, M. J. Beelen<sup>3</sup>, G. J. L. Naus<sup>3</sup>, M. P. Simunovic<sup>1,2</sup>, M. Latasiewicz<sup>2</sup>, A.D. Farmery<sup>4</sup>, M. D. de Smet<sup>3</sup>, and R. E. MacLaren<sup>1,2,\*</sup>

<sup>1</sup>Nuffield Laboratory of Ophthalmology, Department of Clinical Neurosciences, University of Oxford, Oxford, United Kingdom <sup>2</sup>Oxford Eye Hospital, Oxford University Hospitals NHS Foundation Trust, Oxford, United Kingdom <sup>3</sup>Preceyes BV, Eindhoven, the Netherlands <sup>4</sup>Nuffield Division of Anaesthetics, University of Oxford, Oxford, United Kingdom

### Abstract

Microsurgery of the retina would be dramatically improved by instruments that offer supra-human precision. Here, we report the results of a first-in-human study of remotely controlled robot-assisted retinal surgery performed through a telemanipulation device. Specifically, 12 patients requiring dissection of the epiretinal or inner limiting membrane over the macula were randomly assigned to either undergo robot-assisted-surgery or manual surgery, under general anaesthesia. We evaluated surgical success, duration of surgery and amount of retinal microtrauma as a proxy for safety. Surgical outcomes were equally successful in the robotic-surgery and manual-surgery groups. Differences in the amount of retinal microtrauma between the two groups were statistically insignificant, yet dissection took longer with robotic surgery (median time, 4 min 5 s) than with manual surgery (1 min 20 s). We also show the feasibility of using the robot to inject recombinant tissue plasminogen activator under the retina to displace sight-threatening haemorrhage in three patients under local anaesthesia. A safe and viable robotic system for intraocular surgery would enable precise and minimally traumatic delivery of gene therapy or cell therapy to the retina.

### Key terms

Robotic; retina; surgery; intraocular; telemanipulation

---

\*Correspondence: Nuffield Laboratory of Ophthalmology, Level 6 West Wing, John Radcliffe Hospital, Oxford University Hospitals NHS Foundation Trust, Headley Way, Oxford OX3 9DU, United Kingdom.

#### Data Availability Statement

The authors declare that all data supporting the findings of this study are available within the paper and its supplementary information.

**Author contributions:** TLE: surgeon, study design, participant recruitment, manuscript writing and review; KX: participant recruitment, study design, data recording, figure construction, manuscript writing and review; HCMM and MJB: robotics/software engineers, design and constructions of the PRECEYES Surgical System, robot system training, study design and implementation, movie editing, manuscript writing and review; GJLN: study design, manuscript writing and review; MPS: study design, manuscript review; ML: surgeon, manuscript review; ADF: anaesthetist, manuscript writing and review; MDDS: design and clinical translation of PRECEYES Surgical System, manuscript writing and review; REM: chief surgeon and principal investigator, manuscript writing and review.

**Competing interests:** TLE, KX, ML, REM, MPS, ADF – no relevant conflict of interest; HCMM, MJB, GJLN – robot engineering and development at Preceyes B.V., Eindhoven, the Netherlands (employment); MDdS – (shareholder in Preceyes B.V.).

## Introduction

Retinal surgery requires some of the finest instrument manipulations in the field of microsurgery, yet the theoretical advantages of robotic interface in terms of tremor-filtering and precision have not been applied to intra-ocular surgery to date. In conventional vitreo-retinal (VR) surgery, the surgeon approaches the retina through a ‘key-hole’ set-up with fine handheld microsurgical instruments (<1 mm in diameter) passing through cannulae placed at the pars plana (via sclerostomies) while looking down an operating microscope. Over the past four decades, the range of retinal conditions managed surgically has expanded with advances in instrument technology to include retinal detachment, macular hole and epiretinal membrane, such that an emerging limit to further innovation is surgeon physiology. For instance, while the surgeon routinely needs to engage a needle tip or a pair of forceps with the thin (<20 µm) inner limiting membrane (ILM) of the retina without damaging deeper structures, human physiological tremor is present in the order of 100 µm when transmitted to the instrument tip<sup>1–3</sup>. Robotic assistance can overcome physiological barriers by eliminating involuntary movements such as tremor, jerk and low frequency drift. This would facilitate the development of new intra-ocular procedures requiring supra-human levels of precision, as well as improving the safety of existing surgical manoeuvres.

Robotic assistance in eye surgery was first investigated in the 1980s by Spitznas<sup>4</sup>, Guerrouad and Vidan<sup>5</sup>. The eye’s small volume, approximately 6 cm<sup>3</sup><sup>6</sup>, rotational mobility within the socket and delicate internal architecture present unique challenges that preclude the use of bulkier commercially available robotic systems such as the Da Vinci Surgical System (Intuitive Surgical, California USA), and necessitate a dedicated ocular robotic surgical system. These can be classified into four main categories. First, hand-held surgical tools<sup>7,8</sup>, which focus on improved steadiness. Second, co-manipulation control systems<sup>9,10</sup>, which focus on tremor filtering but lack motion scaling and are unable to execute motion profiles or place safety bounds. These can also introduce significant inertial and frictional forces that limit application in dynamic tasks. Third, telemanipulation systems<sup>11–13</sup>, which are often embodied within a console-based setting to provide tremor filtering and motion scaling. Finally, magnetically controlled micro-robots which could provide an alternative surgical approach<sup>14</sup> but lack most benefits of robot assistance. The surgical robotic system (Preceyes BV, Eindhoven, the Netherlands) used in this study is a telemanipulation robot, which had undergone successful animal trials for intra-ocular application<sup>15–17</sup>. The system couples a motion controller held by the surgeon with an instrument manipulator, which can be fitted with an array of standard microsurgical instruments<sup>15</sup>. Features include tremor filtering, dynamic motion scaling, adjustable virtual boundary, and a clutch mechanism that could freeze the position of the instrument inside the eye. The system has previously demonstrated the ability to cannulate and deliver drug into retinal venules (approximately 80 µm in diameter) in the pig eye, a task beyond the capability of manual surgery<sup>15,16</sup> (see Supplementary material).

We conducted a double-armed randomized clinical investigation comparing robot-assisted versus manual retinal surgery in patients undergoing removal of retinal membranes, either epiretinal membrane (ERM) or internal limiting membrane (ILM). These surgical

procedures were deemed good test models for assessing the feasibility and safety of integrating robotic assistance into an ophthalmic operating theatre because they are routine procedures that involve well defined, high precision steps; not because current manual techniques for these particular operations necessarily exhibit shortcomings in accuracy or precision. Epiretinal membrane can cause metamorphopsia or blurred central vision due to distortion of the normal foveal contour. The membrane itself has a mean thickness of 61  $\mu\text{m}$  ( $\pm 28$ )<sup>18</sup>. The ILM is the innermost acellular layer of the retina ( $< 20 \mu\text{m}$  thick) and is circumferentially peeled around a full thickness macular hole (FTMH) to promote its closure and thereby reverse central vision loss<sup>19</sup>. The robotic-assisted surgeon was compared to manual surgery alone for the step requiring maximal instrument precision: lifting a flap of ERM or ILM away from the macula surface using a beveled needle or 'pick'. To simulate its potential future application in subretinal gene therapy, we then used the robot to perform subretinal injection of recombinant tissue plasminogen activator (rt-PA, Alteplase, Boehringer-Ingelheim, Germany) in three patients with acute central vision loss due to subretinal haemorrhage secondary to age-related macular degeneration (AMD). The study was granted national research ethics approval ([Clinicaltrials.gov](https://clinicaltrials.gov) ID: NCT03052881) and was conducted in accordance with the 2013 (7<sup>th</sup> Edition) Declaration of Helsinki.

## Results

### Participants and surgeons

Twelve patients needing either removal of an ERM or ILM peel for macular hole repair were recruited into the clinical study (Table 1). The mean ages were 62 years ( $SD=10$ ) and 72 years ( $SD=8$ ) in the robot ( $n=6$ , 4 males, 2 females) and control ( $n=6$ , 1 male, 5 females) groups respectively. The robot group contained four ILM and two ERM peels, whereas the control group comprised two ILM and four ERM peels. Both right eye robot cases were performed by a right-handed surgeon (REM) who also performed one left eye operation, the remaining three left eye robot cases were performed by a left-handed surgeon (TLE). Four control operations were performed by TLE, one by REM and one by ML. Six further patients requiring emergency displacement of sub-macular haemorrhage were recruited for robot-assisted delivery of rt-PA into the sub-retinal space, randomised to either manual or robot-assisted injection and performed (by REM) under local anaesthesia. Their mean ages ( $SD$ ) were 79 (7) and 85 (6) years respectively.

### Workflow

The normal surgical workflow was not disrupted by installation and sterile draping of the surgical robot, which was performed prior to the patient coming into theatre (Fig. 1). The surgeon and assistant sat in their regular positions at the head of the operating table (Alphastar, Maquet Holding BV & Co, KG, Rastatt, Germany) to which the robotic system was mounted as part of a customised head-rest attachment (Fig. 2). The combined weight of both units was 22 kg. The active robotic part, weighing 3.4 kg, was located on the temporal side of the eye undergoing surgery. Visualisation of the retina and intraoperative optical coherence tomography (OCT) were provided by a Zeiss Rescan 700 operating microscope (Carl Zeiss Meditec AG, Jena, Germany) (Fig. 3). The hybrid approach allowed task-based usage of the robot, i.e. intra-operative switching from manual to robot-assisted steps could

be made within seconds, and the surgeon was able simultaneously to operate the robot with one hand while manipulating a handheld instrument (e.g. the collimated endo-light source, or 'light pipe') with the other hand. When retracted, the robotic system did not impinge on the surgical field, for instance during, application of sterilizing solution to the eye surface and surrounding skin, placement of trocars through the sclera, vitrectomy and wound closure.

### Virtual z boundary

A higher degree of instrument stability and precision of movement was obtained using the robot, particularly in the *z*-axis, perpendicular to the retina. This was facilitated by use of the integrated virtual 'z-boundary' function, which allowed small incremental advancements of the pick (MedOne Surgical Inc, Sarasota, USA) in steps as small as 10  $\mu\text{m}$  until it touched down on the membrane surface. Once in position, an operator-imposed limit to further *z*-axis advancement helped to prevent iatrogenic retinal trauma during lateral movements of the beveled tip of the pick to raise a flap of membrane (Supplementary video S1). As a further refinement, during the *x* and *y*-axis instrument movements on the retinal surface, automated software-derived adjustments in the *z*-axis compensated for the eye's radius of curvature, thus preventing inadvertent retinal touch during lateral movements of the instrument tip. Virtual *z*-boundary also enabled the rt-PA cannula to penetrate the retina and enter the subretinal space in a highly controlled manner by advancing in small increments commensurate with known retinal thickness once the cannula had been positioned on the retinal surface.

### Stability of the eye in robot-assisted cases

Despite observing near complete stillness of the instrument in robot-assisted cases in contrast to manual controls, some relative movement of the robot-manipulated instrument was observed even under general anaesthesia due to rotational forces transmitted to the eye by the hand-held light pipe (Supplementary video S1). To negate this effect, a static trans-scleral light source (chandelier illumination, Constellation Vision System, Alcon Inc, Fort Worth, USA) was used in cases 5 and 6 (Supplementary video S2). This arrangement further improved stillness in the surgical field to the extent that it tended to unmask patient movements never usually observed in manual retinal surgery, such as ocular pulsations secondary to the heartbeat, or slow rhythmic cyclotortions of the eye under general anaesthesia.

### Comparison of robot-assisted versus manual membrane peeling

The median time (min:sec) to move a pick from the anterior vitreous cavity to a position over the macula, i.e. safely poised ready to engage with the membrane, was 00:12 (IQR 0:04) for the control group and 2:26 (IQR 2:52) for the robot group ( $p=0.002$ ) (Fig. 4). The median time (min:sec) to complete raising a flap of either internal limiting or epiretinal membrane with the pick in the control and robot groups was 1:20 (IQR 0:58) and 4:55 (IQR 2:20) respectively ( $p=0.06$ ). The mean total duration of surgery (defined by the interval between inserting the first trocar into the sclera and injecting subconjunctival antibiotic prior to removal of the eyelid speculum) was 31 min (95% CI 27 – 35) and 55 min (51 – 60) for the control and robot groups respectively ( $p<0.0001$ ). The final anatomical outcomes were

equally successful in the robot and control eyes with closure of macular holes and removal of ERM in all cases as evidenced by spectral-domain OCT (Spectralis, Heidelberg Engineering, Heidelberg, Germany) (Fig. 5).

The amount of iatrogenic retinal micro-trauma during robot-assisted or manual surgeries, defined as retinal touches (which resulted in localised blanching) and micro-haemorrhages (retinal touches which further resulted in localized bleeding), were quantified by the surgical assistant and supported by video recordings. The median (range) number of iatrogenic retinal touches or micro-haemorrhages in the control group was 1 (0 – 2) compared with 0 (0 – 2) in the robot group (Fig. 4). There was no statistically significant difference between the two treatment groups ( $p=0.2$ ).

### Return to position functionality

During robot-assisted surgery, the robot user interface allowed surgeons to store the three-dimensional location of an instrument inside the eye. Subsequent activation of the ‘return to position’ function would automatically restore the instrument to its original location i.e. without requiring directional input from the surgeon. The speed of instrument movement was under surgeon control via a foot pedal, and robot movements could be overruled at any time. The software-guided instrument first aimed at the stored target position ( $x/y$  movement) and underwent axial rotation, before advancing along its  $z$ -axis until the stored position was reached.  $Z$ -axis movements were automated to proceed through two speed phases: the instrument could be moved quickly initially, before automatically transitioning to a slower top speed within 2 mm of the final position, allowing the surgeon sufficient response time when close to the retina. On all attempts at return to saved position in the robot-assisted surgeries, the instrument tip was successfully returned to the correct retinal landmark without the need for further manipulation.

### Subretinal injection of rt-PA

Having validated the safety of the robotic system under general anaesthesia in the first six patients, the next phase of the study involved giving subretinal injection to three more patients under local anaesthesia. Since the indication for surgery was submacular haemorrhage, a complication of age-related macular degeneration, the patients undergoing this procedure were generally elderly and would ordinarily have a local anaesthetic (regional block). The procedure involved robot-assisted delivery of 0.025 to 0.10 ml (depending on the size of the haemorrhage) of a 200  $\mu\text{g/ml}$  recombinant tissue plasminogen activator (rt-PA) solution (Alteplase, Boehringer Ingelheim, Germany) under the retina, which followed as closely as possible the standard manual approach<sup>20</sup> first described by Peyman et al<sup>21</sup>. The instrument manipulator was then docked to the conical scleral port adaptor on the eye and the needle advanced through the port into the vitreous cavity. The instrument manipulator was used to move the cannula tip towards the retinal surface under visual and intra-operative OCT guidance (Zeiss Rescan 7000, Carl Zeiss Meditec AG, Jena, Germany) until it was within 100  $\mu\text{m}$  of the retinal surface, immediately above the injection site adjacent to the submacular haemorrhage. To facilitate controlled cannula entry into the tissue plane between the retina and the underlying retinal pigment epithelium (RPE), 20–50  $\mu\text{m}$  incremental advancements (‘nudges’) in the  $z$ -axis were performed using the robotic

instrument manipulator to a pre-defined depth consistent with retinal thickness (around 250  $\mu\text{m}$ ) before initiation of subretinal injection (Supplementary video S3).

In one of the three patients who received robot-assisted rt-PA injections, transient intra-operative exacerbation of cataract precluded a clear view of the cannula tip against the retina. The subretinal injection was completed manually by rotating the eye so as to move the lens opacity away from the visual axis. The subretinal injections were otherwise completed successfully in all patients. The injection durations (min:sec) were 8:31 and 3:12 for the robot group and 4:00, 6:32 and 4:22 for the control group (Table 2). An air bubble was inserted at the end of the operation with instructions for the patient to sit up at 45° overnight, which resulted in pneumatic displacement of the thrombolysed blood (Table 2).

## Discussion

In this study, we report the first use of a remotely controlled electronic robotic device to perform high precision surgery inside the human eye. Using common retinal procedures, we thus provide proof-of-concept for the use of robotic assistance in intraocular surgery. Safety was demonstrated in two procedures: i) by using a sharp metallic tip to lift a membrane from the inner surface of the retina (with the z-axis limiter engaged to limit retinal touch), and ii) by using the z-axis control to advance a fine cannula through the retina into the subretinal space, thus allowing controlled delivery of a drug into the correct tissue plane. These operations were chosen not because they are obvious candidates for enhanced performance with robotic assistance, but because they are common vitreoretinal procedures that are familiar to all vitreoretinal surgeons, which additionally require high precision instrument manipulation. Furthermore, subretinal delivery of rt-PA was a good model for future robot-assisted retinal gene therapy. In this setting, the ability to pause the instrument tip position in 'standby mode' to allow a slow 'drip feed' subretinal infusion in place of a rapid 'pressure jet' retinal detachment would make it an arguably safer technique. This would be particularly relevant when operating on eyes affected by an inherited retinal degeneration. Whilst robot-assisted surgery was typically slower than manual surgery for all participants, in all cases safety took precedence over speed. Fewer inadvertent retinal touches and resulting micro-haemorrhages were observed in the robot cases compared to controls, and whilst this did not reach statistical significance, the absence of any obvious difference was supportive of the robotic system's safety profile. No system malfunctions were encountered over the nine procedures. The robotic system was generally unobtrusive in the operating theatre, although it did necessitate the surgical assistant switching to the opposite side to make space for the instrument manipulator and motion controller components (Fig. 1).

Robotic surgery provides increased precision and accuracy, standby functionality and the ability to store specific coordinates for future use. These functionalities increase safety, allow the surgery to be limited to specific targets and therefore promise higher efficiency and possibly better outcomes. In general surgery, fully robotic systems were introduced more than a decade ago. The first commercial surgical robot was used in 1985<sup>22</sup>. In 2000, Intuitive Surgical introduced a tele-surgical system coupled to a binocular lens and camera to transmit magnified images of the surgical field; a technology that was rapidly adopted in urology and subsequently in other surgical arenas<sup>23–25</sup>. However, robotic surgery remains



mired in controversy. Precision is increased, but at the cost of longer surgical times, with outcomes often not much different from surgery carried out by well-trained surgeons<sup>26</sup>. The optimal interaction between robots and humans still remains to be defined<sup>27</sup>, while insurers are starting to ask themselves if the added cost is worth it<sup>28</sup>. This environment is a major challenge for the introduction of robotic systems to ophthalmology.

Robotics in ophthalmology must deliver high precision in an anatomically constrained environment. This has led to solutions centered around one of three approaches. Firstly, a direct assist strategy whereby physiologic tremor in handheld instruments is stabilised, thereby enhancing the dexterity of the surgeon<sup>29,30</sup>. The challenge here is that sensing, filtering and compensation have to occur in a single cycle without any phase lag. A second approach is co-manipulation, where a robotic system is designed to co-operatively move an instrument with the surgeon<sup>31</sup>. The degrees of freedom are limited to those required for a specific task, for example cannulation. The surgeon is allowed to adjust resistance and motion in the remaining degrees of freedom as needed to carry out the procedure. A third approach is tele-manipulation, where through a master-slave system a robotic micromanipulator is asked to carry out a series of tasks required by a given procedure<sup>15,32</sup>. The challenge is to program the slave appropriately to carry out or assist intuitively the actions of the surgeon. Of the three systems, the most versatile is certainly a tele-operated system, but it is also the most complex.

In the current robotic system, the physical connection between instrument manipulator and the eye, via a conical dock, was a key design feature that enhanced ocular stability during robotic manoeuvres. By design, the motion of the instrument manipulator pivots around the scleral entry site (at the tip of the conical dock), thereby avoiding any deformational and tractional forces on the globe. When inside the eye, the instrument manipulator/cannula docking connection minimized instrument deflection that could degrade instrument precision e.g. due to axial friction or saccadic eye movements. Another capability of the robotic system was dynamic motion scaling, which actively adapted to instrument position within the eye. Lower motion scaling ratios (1:5) were used for relatively macro-movements at the centre of the eye, whereas higher motion scaling (1:25) was used when the instrument tip was near the retina, thus facilitating the finer instrument movements required for elevating a retinal membrane. The 'return to stored position' function worked precisely without any need for manual override or corrective adjustments to the final instrument position. This unique feature could potentially enable a needle to enter the same hole (retinotomy) in the retina twice without enlarging its size during a two-staged approach to subretinal gene therapy<sup>33</sup>

Unexpected patient head movement can be hazardous during any intraocular surgery if the surgeon is unable to react quickly by withdrawing their instruments. Precautions were taken in this study to minimize the risk of patient movement. In all cases therefore, the forehead was taped to the headrest, and in the robot cases involving membrane peeling, patients underwent general anaesthesia. This was maintained with a total intravenous technique (propofol and remifentanyl) with muscle relaxation, which ensured that spontaneous respiration was abolished. Patients were mechanically ventilated, allowing the rate and depth of each breath to be controlled by the anaesthetist. In addition, although its use was not

required in any cases, the robot system was equipped with a surgeon-initiated automatic retract function capable of ejecting any intraocular instrument along its current axis in less than 500 ms. The hybrid nature of the system also meant that direct tactile feedback to the surgeon was retained if unexpected head movements occurred, e.g. via the handheld second instrument, thus enabling the surgeon to react quickly if required. We subsequently proceed to performing all subretinal injection cases safely under local anaesthetic eye block i.e. without general anaesthesia.

The limitations of this study were its small cohort size and a lack of previous experience with robot-assisted surgery from both surgeons. Using macular hole closure rate as a surrogate for successful ILM peel also carries the caveat that hole closure can occur with vitrectomy and gas tamponade alone. We therefore relied primarily on video recordings of the surgery (e.g. see Supplementary Information) and surgeons' operation reports to establish whether the membrane had been removed. Speed was always sacrificed in the interests of safety, which biased the surgery duration and other timed steps in favor of standard manual technique. Additional intra-operative time was spent during the robot cases on familiarizing surgeons with the system. A major consideration in robotics today is the associated increased surgical time and cost. Both can be reduced if the robotic system can be utilized in an assistive mode, where it is made use of during precision tasks, and parked at safe distance away during other stages of surgery. It should also be adaptable to existing operating room suites, and be as non-obtrusive as possible. For cost effectiveness, a robotic system should also be of use in a variety of different ophthalmic procedures. In this regard, a tele-operated system best meets these requirements, and were some of the design requirements for the Preceyes system. A current challenge is to provide high precision and accuracy with more ease and speed. We encountered limits related to our own human physiologic limitations of depth perception. To increase precision and accuracy, the robot will need to perform tasks in a more automated fashion with the bounds being defined by the operator. To this end, the development of sensing devices that can detect distance on a  $\mu\text{m}$  scale would be useful. Once incorporated into the design of the robot, it will be possible to carry out tasks more quickly as well as with an increased safety margin. Any motion made by the patient could lead to the retraction of an instrument to a safe distance, or outside the eye.

To realize the potential of robotics in ophthalmic surgery the onus lies with surgeons to conceive of potentially sight saving procedures not currently possible in the human eye using standard manual instrument control e.g. cannulation of retinal blood vessels to inject anti-thrombotic agents for the treatment of retinal vascular occlusion<sup>16</sup> or accurate delivery of precise, standardized volumes of novel therapeutic agents such as stem cells or gene therapy into the subretinal space. Further optimisation of workflows and instrumentation will be required before deploying the robotic system for such purposes in the future.

## Methods

### Recruitment and eligibility

Participants were recruited from the vitreoretinal outpatient clinic at the Oxford Eye Hospital. Eligible patients were deemed to require either ERM/ILM peel or subretinal rt-PA



for displacement of a submacular haemorrhage by the consultant ophthalmologist (REM). Informed consent was obtained and the research followed the guidelines of the Declaration of Helsinki (7<sup>th</sup> revision, 2013). A total of 12 patients were recruited and randomised to receive either robot-assisted (n = 6) for standard manual (n = 6) membrane peeling surgery. Similarly, six emergency patients who presented with acute submacular haemorrhage were recruited for subretinal rt-PA injection and randomised to have either robot assistance or standard manual surgery.

### **Anaesthesia**

The first six participants undergoing robot-assisted ERM surgery received an intravenous general anaesthetic using propofol and remifentanyl, plus muscle relaxation and mechanical ventilation, administered by a senior anaesthetist with neuro-anaesthesia experience (ADF). Patients were selected for this part of the study on the basis that they would be suitable for general anaesthesia. Medical tape was applied across the forehead of all participants to minimize the risk of unexpected head movement. The three patients undergoing subretinal injection of rt-PA had local anaesthetic applied as a sub-tenon injection of up to 10 ml of a 50:50 mixture of 1% lignocaine and 2.5% bupivacaine. No sedation was required in these three patients.

### **Training**

Prior to using the robotic system in surgery, all surgical personnel (surgeons, assistants and nursing staff) underwent a dedicated training protocol. This was divided in three sessions comprising the use of the device on an artificial eye, validating safety functionalities, evaluating the surgical protocol and assessing the predicted impact on the normal surgical workflow. Particular attention was given to the execution of safety procedures, as well as proficiency in the installation and sterile draping of the device.

### **Recording outcome variables**

The duration of robot and control membrane peel surgeries was recorded. Duration of two other specific intra-operative tasks was also recorded: i) moving the pick instrument from the anterior vitreous cavity e.g. just inside the eye, to a position over the retinal surface, and ii) initiation of the membrane flap with the pick. The number of iatrogenic retinal touches and resulting haemorrhages were recorded as well as the surgeons' descriptive experiences. All relevant recorded data are presented in the Results section. Clinical data are presented in accordance with data protection policies of the UK National Research Ethics Service.

### **Robotic surgical system**

The robotic surgical device was custom built for this clinical investigation in compliance with 93/42/EEG, based on a dedicated proof-of-concept system<sup>15,16</sup> and does not have a CE Mark. The device consisted of a 4-axis motion controller (motion controller) for hand motion input by the surgeon, and a 4-axis instrument manipulator/holder (instrument manipulator) that enabled instrument movement. When the clutch on the motion controller (motion controller) was engaged by simultaneous thumb and index finger pressure over two switches on the joystick, coupling between the motion controller and instrument manipulator

was activated. Once coupled, the instrument manipulator replicated the surgeon's movements of the motion controller joystick with dynamic scaling depending on instrument tip position within the eye. Additional tremor filtering was added as needed using a programmed protocol. When the clutch was disengaged, the instrument manipulator maintained its current static position ('standby' functionality). Careful pre-operative patient positioning on the operating table was required to place the remote center of motion (RCM) of the robot within reach of the operated eye.

### Surgical technique

After standard manual 23 gauge (G) three port pars plana vitrectomy and staining of the membrane with MembraneBlue Dual (DORC BV, Zuidland, the Netherlands), the conical tip of the instrument manipulator was docked to a customised conical-shaped scleral port adaptor. The apical end of the adaptor was designed to fit over a standard 23 G trans-scleral valved trocar (Alcon Inc, Forth Worth, USA). This arrangement secured the eye firmly in primary position while allowing the instrument manipulator to retract from the eye immediately if required. For the ERM/ILM peels, the pick was advanced into the eye by passing through the aligned apices of the two docked conical elements, through the valved port, and into the vitreous cavity. Following 23 gauge standard vitrectomy, a Teflon-tipped retractable 41 G cannula (DORC BV, Zuidland, the Netherlands) was connected to a 1 ml Luer lock syringe (Beckton Dickinson, Oxford, UK) containing 200 µg per ml of rt-PA mounted on the instrument manipulator and connected to the viscous fluid control (VFC) port of the Alcon Constellation Vision System (Alcon, Fort Worth, USA)<sup>33,34</sup>. Injection of subretinal rt-PA was performed adjacent to the submacular haemorrhage. Care was taken to position the 41 G cannula tip precisely in the potential tissue plane between the neurosensory retina and RPE before injection of the drug. Subsequently, the eye was filled with air tamponade to promote displacement of the thrombolysed blood away from the macula.

Initiation of ERM/ILM peeling required the surgeon to make a slit in the membrane with a 23 G pick (MedOne Surgical, Inc., Sarasota, USA) and lifting up a flap. This was generally done within the horizontal raphe in the temporal macula, as it minimizes potential disruption to the retinal nerve fibres from any surgical trauma. The time to raise a membrane flap was taken from when the surgeon commenced a first attempt (manual or robot-assisted) at engaging the macular membrane with the pick, and concluded once the surgeon determined that a flap of sufficient size (to allow grasping with vitrectomy forceps) had been raised.

To test the 'return to position' function of the robotic surgical system after membrane peeling, the pick was moved to the anterior vitreous cavity after first storing its position over the raised flap or a nearby vascular landmark. 'Return to position' mode was then activated and a record made of any compensatory instrument movements required after automated return of the instrument to the saved position in three-dimensional space within the eye.

### Statistics

The time to initiate membrane flap or position an instrument over the retina were non-normally distributed, and hence these data were presented as median with interquartile range

(IQR) and a Mann-Whitney unpaired t-test was performed to compare these parameters (GraphPad Prism version 6.0 for Mac, GraphPad Software, La Jolla, California, USA) between robot and control groups. A Mann-Whitney test was also applied to comparison of the number of iatrogenic retinal micro-trauma events, which were similarly non-parametric in distribution. Total duration of surgery was normally distributed and thus mean and 95% confidence intervals describe these data together with an unpaired Student's t-test to determine the significance of difference between robot and manual groups.

## Supplementary Material

Refer to Web version on PubMed Central for supplementary material.

## Acknowledgments

**Funding:** The National Institute for Health Research (NIHR) Oxford Biomedical Research Centre, Zien Zonder Zorgen (ZIZOZ) – a Dutch charity, and the Nuffield Medical Fellowship. UK National Research Ethics Service approval ref: 16/LO/005).

**Study sponsor:** The study was sponsored by the University of Oxford.

## References

1. Eshner AA. A graphic study of tremor. *J Exp Med.* 1897; 2:301–312.
2. Harwell RC, Ferguson RL. Physiologic tremor and microsurgery. *Microsurgery.* 1983; 4:187–192. [PubMed: 6669016]
3. Riviere CN, Rader RS, Khosla PK. Characteristics of hand motion of eye surgeons. *Engineering in Medicine and Biology Society, 1997. Proc. 19th Annual International Conference of the IEEE* 1690–1693; IEEE; 1997.
4. Spitznas M. Motorized Teleguided Stereotactic Micromanipulator for Vitreous Microsurgery. *Arch Ophthalmol.* 1983; 101:623–630. [PubMed: 6838423]
5. Guerrouad A, Vidal P. SMOS: stereotaxical microtelem manipulator for ocular surgery. *Images of the Twenty-First Century. Proc. Annual International Engineering in Medicine and Biology Society* 879–880; IEEE; 1989.
6. Silver DM, Csutak A. Human Eye Dimensions for Pressure-Volume Relations. Vol. 51. IEEE; 2010. 5019
7. Wei Tech AngRiviere CN, Khosla PK. Design and implementation of active error canceling in hand-held microsurgical instrument. *Proc. 2001 IEEE/RSJ International Conference on Intelligent Robots and Systems. Expanding the Societal Role of Robotics in the Next Millennium* 1106–1111; IEEE; 2001.
8. Stetten G, et al. Hand-held force magnifier for surgical instruments. *Information Processing in Computer-Assisted Interventions. Lecture Notes in Computer Science.* Taylor RH, Yang G-Z, editors Vol. 6689. Springer; Berlin, Heidelberg: 2011. 90–100.
9. Taylor R, et al. A Steady-Hand Robotic System for Microsurgical Augmentation. *The International Journal of Robotics Research.* 1999; 18:1201–1210.
10. Uneri A, et al. New steady-hand eye robot with micro-force sensing for vitreoretinal surgery. *Proc IEEE RAS EMBS Int Conf Biomed Robot Biomechatron.* 2010; 2010:814–819. [PubMed: 21461178]
11. Nakano T, Sugita N, Ueta T, Tamaki Y, Mitsuishi M. A parallel robot to assist vitreoretinal surgery. *International Journal of Computer Assisted Radiology and Surgery.* 2009; 4:517–526. [PubMed: 2003328]
12. Rahimy E, Wilson J, Tsao T-C, Schwartz S, Hubschman J-P. Robot-assisted intraocular surgery: development of the IRISS and feasibility studies in an animal model. *Eye.* 2013; 27:972–978. [PubMed: 23722720]

13. Meenink HCM, , et al. A master-slave robot for vitreo-retinal eye surgery. In: Spaan H, , et al., editors Proceedings of the 10th International Conference of European Society for Precision Engineering and Nanotechnology; Bedford, UK: Delft Netherlands, EUSPEN; 2010. 408–411.
14. Kummer MP, et al. OctoMag: An Electromagnetic System for 5-DOF Wireless Micromanipulation. *IEEE Trans Robot.* 2010; 26:1006–1017.
15. de Smet MD, et al. Robotic Assisted Cannulation of Occluded Retinal Veins. *PLoS ONE.* 2016; 11:e0162037. [PubMed: 27676261]
16. de Smet MD, et al. Release of experimental retinal vein occlusions by direct intraluminal injection of ocriplasmin. *Br J Ophthalmol.* 2016; 100:1742–1746. [PubMed: 27688592]
17. Meenink T, Naus G, de Smet M, Beelen M, Steinbuch M. Robot assistance for micrometer precision in vitreoretinal surgery. *Invest Ophthalmol Vis Sci.* 2013; 54:5808.
18. Wilkins JR, et al. Characterization of epiretinal membranes using optical coherence tomography. *Ophthalmology.* 1996; 103:2142–2151. [PubMed: 9003350]
19. Kelly NE, Wendel RT. Vitreous surgery for idiopathic macular holes. Results of a pilot study. *Arch Ophthalmol.* 1991; 109:654–659. [PubMed: 2025167]
20. Olivier S. Subretinal recombinant tissue plasminogen activator injection and pneumatic displacement of thick submacular hemorrhage in Age-Related macular degeneration. *Ophthalmology.* 2004; 111:1201–1208. [PubMed: 15177972]
21. Peyman GA, et al. Tissue plasminogen activating factor assisted removal of subretinal hemorrhage. *Ophthalmic Surg.* 1991; 22:575–582. [PubMed: 1961614]
22. Wedmid A, Llukani E, Lee DI. Future perspectives in robotic surgery. *BJU International.* 2011; 108:1028–1036. [PubMed: 21917107]
23. Sim HG, Yip SKH, Cheng CWS. Equipment and technology in surgical robotics. *World J Urol.* 2006; 24:128–135. [PubMed: 16538515]
24. Morel P, et al. Robotic versus open liver resections: A case-matched comparison. *Int J Med Robot.* 2017; 13:e1800.
25. Chen YJ, et al. Outcomes of robot-assisted versus laparoscopic repair of small-sized ventral hernias. *Surg Endosc.* 2017; 31:1275–1279. [PubMed: 27450207]
26. Ahmad A, Ahmad ZF, Carleton JD, Agarwala A. Robotic surgery: current perceptions and the clinical evidence. *Surg Endosc.* 2017; 31:255–263. [PubMed: 27194264]
27. Hiatt LM, Narber C, Bekele E, Khemlani SS, Trafton JG. Human modeling for human–robot collaboration. *The International Journal of Robotics Research.* 2017; 36:580–596.
28. Milne V, Tierney M, Doig C. [Accessed: 19 February 2018] Is robotic surgery worth the cost?. 2016. <http://healthydebate.ca> Available at: <http://healthydebate.ca/2016/10/topic/robotic-surgery>
29. Veluvolu KC, Tatinati S, Sun-Mog Hong, Wei Tech Ang. Multistep Prediction of Physiological Tremor for Surgical Robotics Applications. *IEEE Trans Biomed Eng.* 2013; 60:3074–3082. [PubMed: 23771303]
30. Gonenc B, , et al. Towards robot-assisted vitreoretinal surgery: force-sensing micro-forceps integrated with a handheld micromanipulator. 2014 IEEE International Conference on Robotics and Automation (ICRA) 1399–1404; IEEE; 2014.
31. Gijbels A, , et al. Experimental validation of a robotic comanipulation and telemanipulation system for retinal surgery. 5th IEEE RAS/EMBS International Conference on Biomedical Robotics and Biomechatronics 144–150; IEEE; 2014.
32. Meenink HCM, , et al. Medical Robotics: Minimally Invasive Surgery Woodhead Publishing Series in Biomaterials, no. 51. Gomes P, editor Cornwall: Woodhead; 2012. 185–209.
33. Xue K, Groppe M, Salvetti AP, MacLaren RE. Technique of retinal gene therapy: delivery of viral vector into the subretinal space. *Eye.* 2017; 31:1308–1316. [PubMed: 28820183]
34. Fischer MD, Hickey DG, Singh MS, MacLaren RE. Evaluation of an Optimized Injection System for Retinal Gene Therapy in Human Patients. *Hum Gene Ther Methods.* 2016; 27:150–158. [PubMed: 27480111]

### Summary

A first-in-man robot-assisted device for intra-ocular surgery demonstrating successful peeling of retinal membranes and injection of therapeutic drug under the retina.

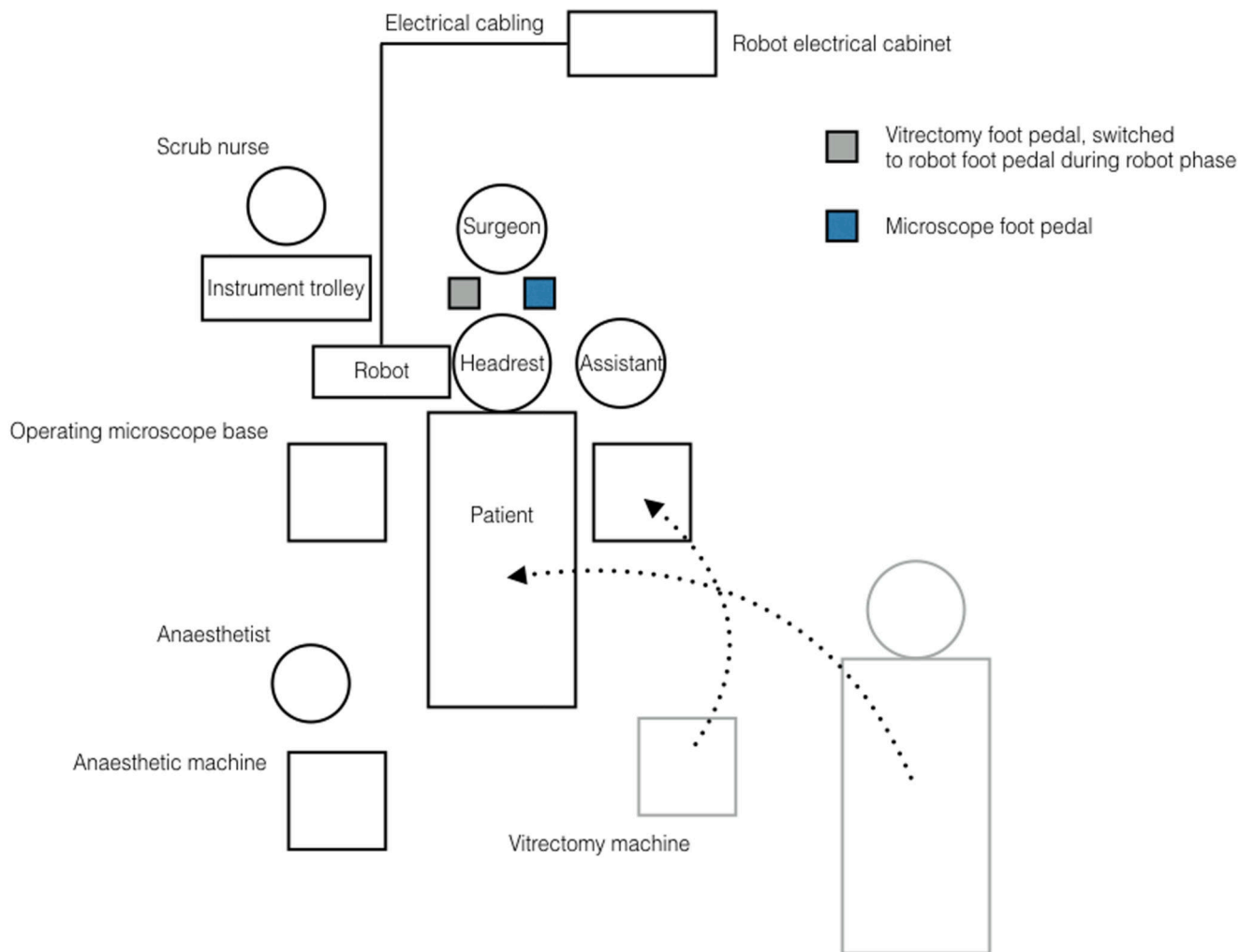


**Figure 1. Operating room floor plan for a right-eye patient.**

The patient was transferred from a trolley bed onto the operating table before the vitrectomy machine was repositioned. Both surgeon and assistant viewed the eye through an operating microscope, with the assistant positioned on the opposite side to the eye undergoing the operation. Careful positioning of the patient was required before the case began to align the eye with the remote centre of motion of the robot.



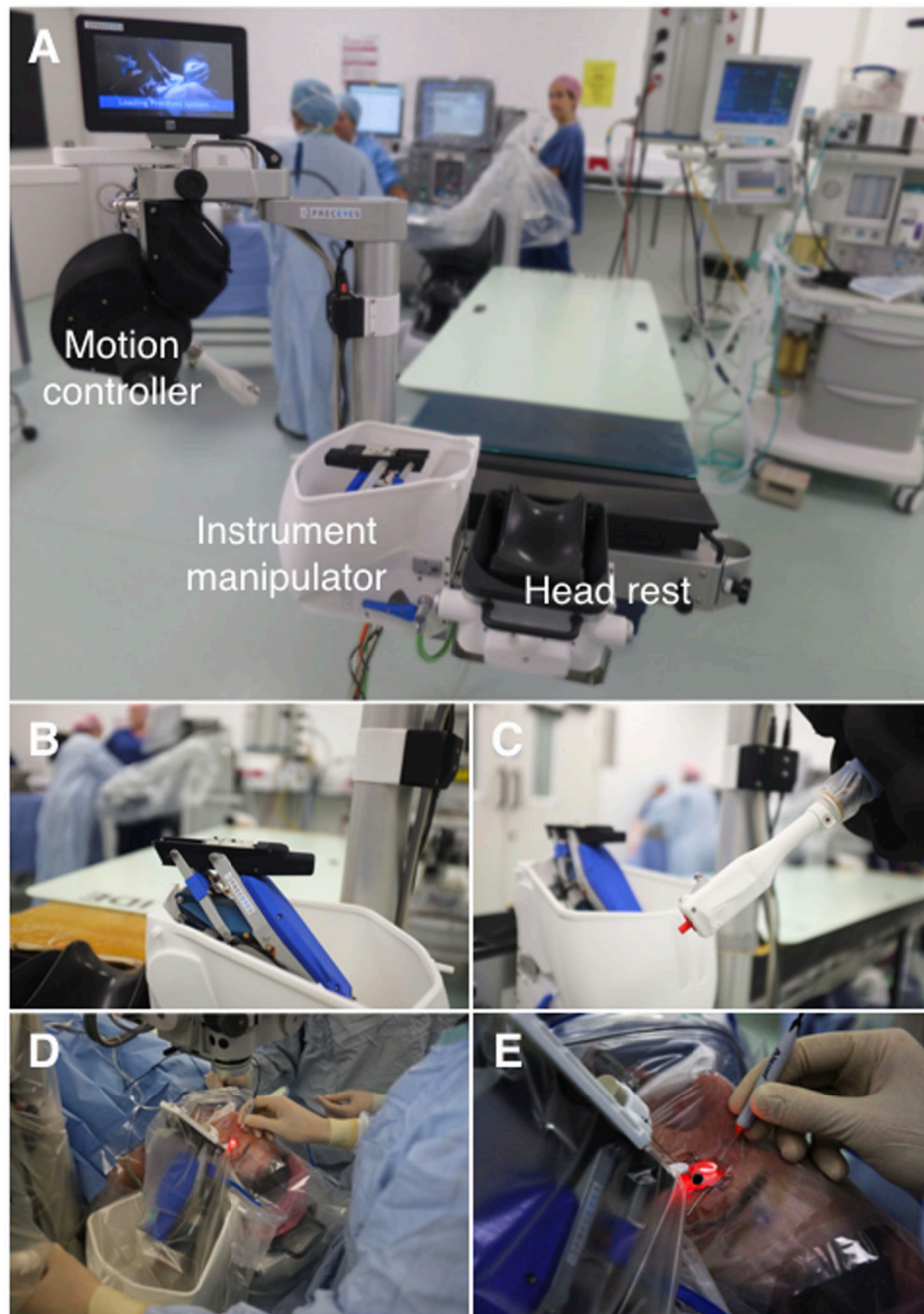


**Figure 2. Robotic set-up.**

(A) The robot system in position at the head of the operating table. Three main components of the robotic system include (B) an instrument manipulator mounted to the head rest, (C) a motion controller and (A) a table-mounted head rest. (D-E) The motion controller is manipulated in four axes ( $x$ ,  $y$ ,  $z$  and rotational) while the surgeon's elbow and forearm is stabilised on the arm of the operating chair. With the clutch mechanism engaged – protruding grey switch in (C) – movements of the motion controller were mirrored by the instrument manipulator. (D) The sterile drape covered both instrument manipulator and

motion controller. (D-E) The hybrid nature of the surgery allowed the surgeon to hold the endo-illumination (light-pipe) in one hand and to control the instrument manipulator loaded with a surgical instrument using the other hand. A separate electronics cabinet is placed outside the surgical area (see Figure 1).

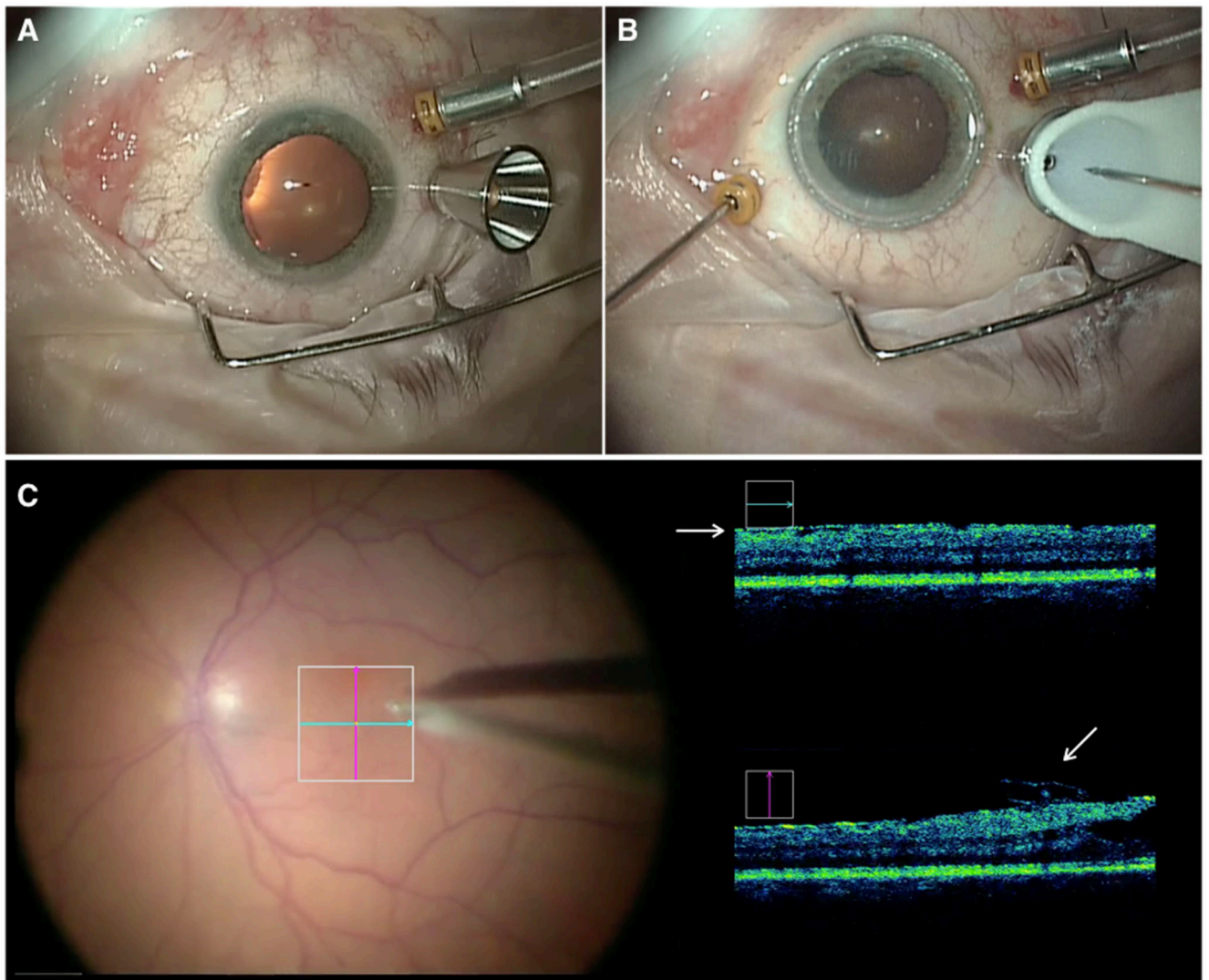


**Figure 3. Docking of the instrument manipulator with the conical scleral port adaptor.**

(A) The metallic conical port adaptor fitted over the standard 23 G valved trans-scleral port (Alcon Inc, Fort Worth, USA), adjacent to the standard fluid infusion line. (B) The sterile white conical tip of the instrument manipulator has docked with the conical port in and the 23 G pick (MedOne Surgical Inc, Sarasota, USA) can be seen as it is advanced towards the eye. The surgeon's left hand was holding the 'light-pipe' endo-illuminator in the eye. (C) The surgeon's view through the operating microscope with live intra-operative optical coherence tomography (OCT) feed (Rescan 700, Carl Zeiss Meditec AG, Jena Germany) showing a flap of epiretinal membrane (ERM) being elevated by the pick in the vertical scan (lower white arrow). The ERM can also be seen in the horizontal scan (upper white arrow).

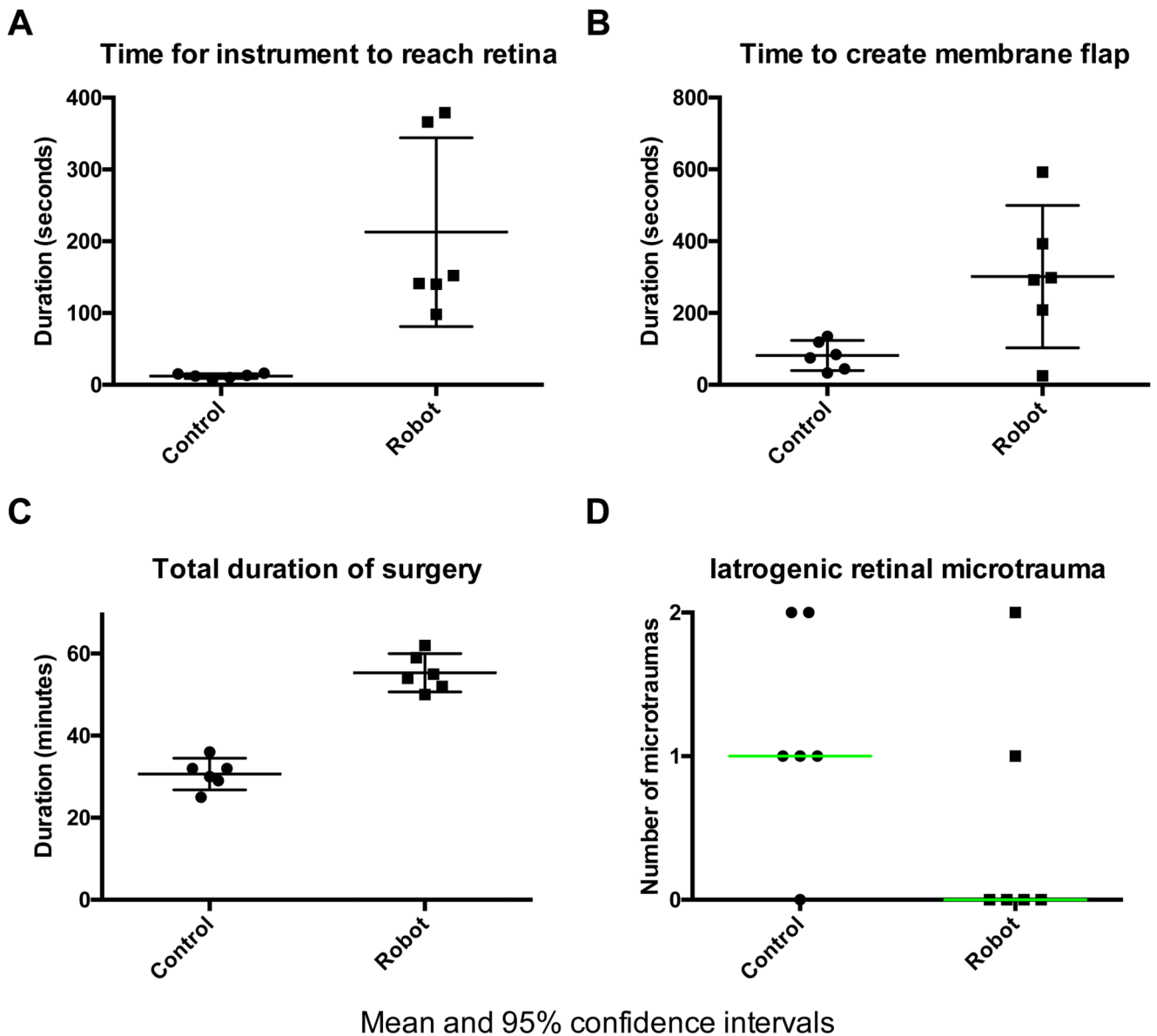


**Figure 4. Objective outcome measures: manual (control) versus robot-assisted retinal membrane peels.**

(A) The median (interquartile range, IQR) time (min:sec) taken to position the 23 G pick close to the retinal surface from its entry point into the eye was 2:26 (2:52) and 0:12 (0:04) in the robot ( $n = 6$ ) and control ( $n = 6$ ) eyes respectively ( $p=0.002$ ). (B) The median (IQR) time (min:sec) taken to create an elevated flap of membrane in control and robot eyes was 1:20 (0:58) and 4:55 (2:20) respectively ( $p=0.06$ ). (C) The mean (95% CI) total duration of surgery was significantly longer in robot cases, 55 min (51 – 60) compared to control cases, 31 min (27 – 35) ( $p<0.0001$ ). (D) There was no statistically significant difference in the number of micro-traumas between the robot and control groups. (A-B) Median and errors bars representing the IQR are shown within the scatter plots. Mean and 95% CI are shown in (C). Median (in green) and no error bars in panel (D).



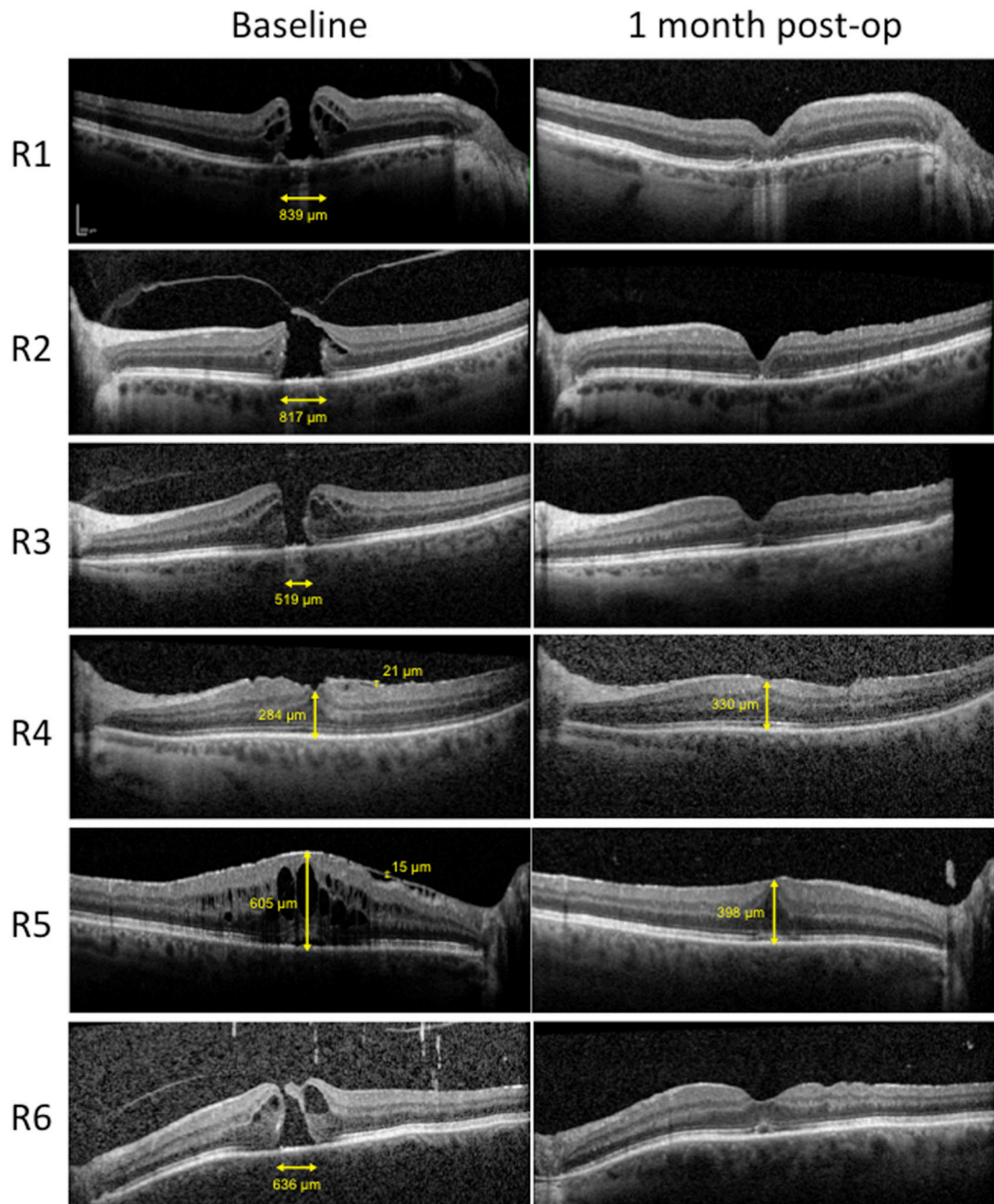


**Figure 5. Pre- and post-operative optical coherence tomography (OCT).**

Spectral domain OCT scans through the central macula showed that participants R1-3 and 6, who underwent robot-assisted inner limiting membrane (ILM) peel, had successful closure of full thickness macular holes. Participants R4-5 underwent robot-assisted epiretinal membrane peels, resulting in reduced retinal distortion (R4) and macular swelling (R5) one month post-surgery. Image scale bars (vertical and horizontal) are shown in the top left panel.

**Table 1**

Clinical details of ERM/ILM peel patients. ERM = epiretinal membrane, ILM = inner limiting membrane, R = right, L = left.

| Participant | Robot/Manual | ILM/ERM | Eye | Age (y) | Successful outcome     |
|-------------|--------------|---------|-----|---------|------------------------|
| R1          | Robot        | ILM     | R   | 71      | Yes (hole closed)      |
| R2          | Robot        | ILM     | L   | 46      | Yes (hole closed)      |
| R3          | Robot        | ILM     | L   | 69      | Yes (hole closed)      |
| R4          | Robot        | ERM     | L   | 53      | Yes (membrane removed) |
| R5          | Robot        | ERM     | R   | 61      | Yes (membrane removed) |
| R6          | Robot        | ILM     | L   | 70      | Yes (hole closed)      |
| C1          | Manual       | ERM     | L   | 62      | Yes (membrane removed) |
| C2          | Manual       | ERM     | R   | 76      | Yes (membrane removed) |
| C3          | Manual       | ERM     | R   | 84      | Yes (membrane removed) |
| C4          | Manual       | ERM     | R   | 71      | Yes (membrane removed) |
| C5          | Manual       | ILM     | R   | 67      | Yes (hole closed)      |
| C6          | Manual       | ILM     | L   | 70      | Yes (hole closed)      |



**Table 2**

Summary of patients who underwent robot-assisted (R1-3) or manual (M1-3) subretinal recombinant tissue plasminogen activator (rt-PA) injection for submacular haemorrhage. HM = hand movements. \*Injection phase of surgery was completed manually due to development of cataract. VA = visual acuity, logMAR = logarithm of the minimum angle of resolution.

| Patient | Age (yr) | Eye   | Pre-op VA (logMAR) | Time taken for injection (min:sec) | Volume injected ( $\mu$ L) | Blood displaced | Post-op VA (logMAR) |
|---------|----------|-------|--------------------|------------------------------------|----------------------------|-----------------|---------------------|
| R1      | 85       | Right | HM                 | 8:31                               | 25                         | Y               | 1.00                |
| R2      | 80       | Right | 0.48               | *                                  | 50                         | Y               | 0.30                |
| R3      | 72       | Left  | 1.18               | 3:12                               | 40                         | Y               | 1.00                |
| M1      | 91       | Right | HM                 | 4:00                               | 100                        | Y               | 0.46                |
| M2      | 85       | Right | HM                 | 6:32                               | 100                        | Y               | 0.30                |
| M3      | 80       | Right | 1.00               | 4:22                               | 100                        | Y               | 0.60                |